metals

MDPI

Article

Hybrid Solder Joints: Viscosity Studies of the Nanocomposite Flux with Fe Nanoparticle Additions

Andriy Yakymovych *, Irina Wodak and Golta Khatibi

Institute of Chemical Technologies and Analytics, TU Wien, 1060 Vienna, Austria; irina.wodak@tuwien.ac.at (I.W.); golta.khatibi@tuwien.ac.at (G.K.)
* Correspondence: andriy.yakymovych@tuwien.ac.at

Abstract: Viscosity is one of the most important physical characteristics of choosing a flux for solder paste. However, not in all cases do the producers give information about the viscosity of commercial flux. A recent promising trend is to mix various kinds of nanoparticles with solder paste or flux and investigate the produced solder joints. However, the impact of nanosized inclusions on the viscosity of the flux has practically not been investigated. In this study, the temperature and shear rate dependencies of the viscosity of the nanocomposite flux were measured. For this purpose, the commercial flux has been mixed with Fe nanoparticles up to 2.0 wt.% of inclusions. It has been shown that viscosity increases with the addition of Fe nanoparticles. However, it is valid only for first heating up to circa 340 K. The viscosity values of the flux with and without nanosized inclusions are practically similar by further heating to 360 K as well as by subsequent cooling. Additionally, the performed differential thermal analysis has shown the heat effects, which are in good agreement with viscosity behavior.

Keywords: flux; metal nanoparticles; shear rate; viscosity

check for updates

Academic Editor: Frank Czerwinski

Received: 3 December 2024
Revised: 9 January 2025
Accepted: 15 January 2025
Published: 18 January 2025

Citation: Yakymovych, A.; Wodak, I.; Khatibi, G. Hybrid Solder Joints: Viscosity Studies of the Nanocomposite Flux with Fe Nanoparticle Additions. *Metals* **2025**, *15*, 93. https://doi.org/10.3390/met15010093

Copyright: © 2025 by the authors. Licensee MDPI, Basel, Switzerland. This article is an open access article distributed under the terms and conditions of the Creative Commons Attribution (CC BY) license (https://creativecommons.org/licenses/by/4.0/).

1. Introduction

Solder paste is widely used in the manufacture of printed circuit boards to connect surface mount components to pads on the board. It consists of flux and solder particles, which are uniformly distributed in the medium (between 80 wt.% and 90 wt.%).

One of the main reasons to use flux as a medium is that it acts as a reducing agent during the soldering process. The flux is used to make the solder flow more easily as well. Acids called "activators" and substances called "vehicles" or "solids" form flux. The first ingredient removes oxides, and the second coats the surface, preventing further oxidation after removing the primary oxides. The minimum temperature at which the acid begins working is the "activation temperature." The activation temperature is often near the temperature of 338 K; it should be noted that it is the starting temperature, and the reaction occurs for a while. In this paper, we focus on the "neutral pH" fluxes, which either produce acids when heated or start with high acidity but are neutralized by the reaction with oxygen at higher temperatures. The separation of the flux medium from the paste occurs during soldering, and the flux residues are easily removed after the process by water.

There is a number of studies related to the investigation of the impact of nanoparticles (NPs) on the viscosity of liquid medium. For instance, nanoparticles increase the viscosity of the nonviscous fluid, such as water, ethylene glycol, or metals [1–3]. Yalçın et al. [4] have postulated that the larger NPs increase the viscosity of water greater than smaller

ones based on the experimental data of the viscosity of the water-based nanofluid viscosity with ZnO nanoparticles varying particle sizes. In contrast, nanoparticles are used in highly viscous liquids as viscosity reducers [5]. Furthermore, it was stated that the addition of a very small amount of metal micro- and nanoparticles such as Co, Cu, Ni, etc., can enhance the wettability of lead-free SnAgCu solders; however, an excessive addition can degrade the wetting property [6]. The literature [7] has investigated the viscosity of the Colombian heavy crude oils HO (heavy oils) and EHO (extra-heavy oils) with ceramic nanoparticles (Al_2O_3, Fe_3O_4, and SiO_2) at concentrations of 10, 100, 1000, and 10,000 mg/L at 298 K at a shear rate range of 1–75 s^{-1}. It is observed that the viscosity tends to decrease by increasing the concentration of nanoparticles in the medium with the optimum concentration of 1000 mg/L.

The present study has been performed within the research project focus on hybrid solder joints, which consist of substrate, solder, and nanocomposite flux. In our previous studies, the mechanical properties and microstructures of the solder joints were widely investigated. For instance, it was demonstrated that minor additions of Fe or ceramic NPs into the soldering flux led to a reduction in the growth of interfacial IMC layers between solder and substrate, and this subsequently improved the mechanical properties of lead-free solder joints [8,9]. The temperature dependence of the wetting angle of the nanocomposite flux with minor additions of Fe nanoparticles was published in [10]. The measured contact angle decreased from about 60° to about 50° at room temperature by the addition of 0.5 wt.% and 1.0 wt.% Fe NPs to the flux. It was shown that the wetting angle decreases with the temperature increase. For instance, the wetting angle of the flux equals 23° at 345 K, while the samples with 1.0 wt.% and 2.0 wt.% Fe NPs have exhibited the contact angle of about 20°. Furthermore, the samples with 0.0 wt.%, 0.5 wt.%, 1.0 wt.%, and 2.0 wt.% Fe-NPs have shown a significant drop in the wetting angle between 318 K and 330 K during heating. In contrast, the shear rate of the viscosity of the nanocomposite flux was investigated only at room temperature. A preparation of hybrid solder joints including Fe NPs can be imagined as a sandwich consisting of the following layers: a Cu plate/flux with a FeNPs/SAC foil/flux with a Fe NPs/Cu plate. Information on the changes in the viscous flow of the flux by additions of Fe NPs is essential to model the processes in the hybrid solder joints during the reflow process. Therefore, it was decided to extend the viscosity investigations including the temperature measurements.

2. Materials and Methods

The nanocomposite fluxes were prepared by mixing nanosized Fe powder (Nanografi, average particle size is about 50 nm) with the commercial flux (Lötfett produced by Stannol), varying the content of nanosized impurities from 0.0 wt.% to 2.0 wt.%. The passivated nanoparticles were analyzed by transmission electron microscopy (TEM/JEOL JEM-2000FX) operated at 200 kV. The micrographs of the samples were taken in the bright-field imaging mode (Figure 1). It was confirmed that metal nanoparticles are covered by an oxide shell, which protects the metal core from being oxidized in air. A visible oxide shell yields an approximate thickness of 5–6 nm. The nanoparticles were first mechanically mixed in the flux for 5 min and then dispersed using an ultrasonic gun.

The viscosity measurements were performed by a plate–plate rheometer (MCR300 SN621304, Anton Paar—Rheoplus/32). The sample was sandwiched between two parallel plates/disks. The top plate rotates, shearing the material between the top plate and the bottom plate, which is held stationary. For instance, a PP-25 stamp was utilized with a radius of 24.95 mm, which was adjusted to a sample height (i.e., plate distance) after applying the flux.

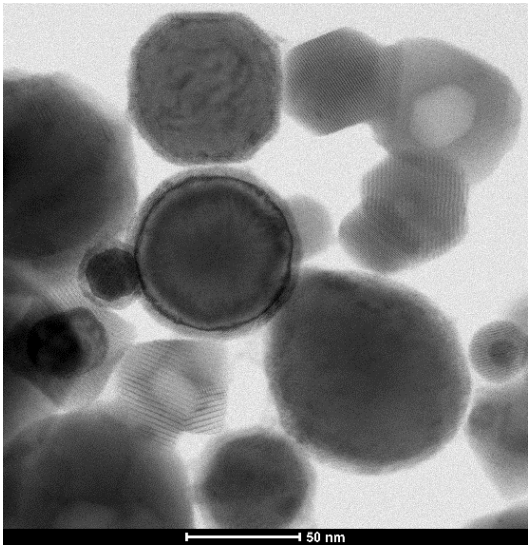


Figure 1. TEM image of Fe nanoparticles.

The sample transmits a torque that can be measured and recalculated into shear strain and shear stress. The viscosity in this case can be expressed as a function of shear stress and the shear rate:

$$\eta = \tau/\gamma, \quad (1)$$

where η is the viscosity in Pa·s, τ is the shear stress in Pa, and γ is the shear rate in s^{-1}.

Each experiment was started with the viscosity measurement at room temperature by increasing the shear rate until 60 s^{-1} or 100 s^{-1} using a logarithmic ramp over a five-second period. Each sample was twice heated and cooled at the highest shear rate. At the end of the experiments, the viscosity was measured at room temperature by decreasing the shear rate.

The differential thermal analysis (DTA) of the flux was performed using Pegasus STA 449C. The measurement was performed under argon flow (50 mL/min) in two runs with the temperature rate of 0.4 K/min and the maximal temperature of 363 K. The sample was placed in the AlOx crucible.

3. Results and Discussion

The primary investigations performed at room temperature showed a significant decrease in viscosity by the shear rate increase, especially in the range between 0 s^{-1} and 10 s^{-1}, with an abrupt drop of viscosity values up to four times from the initial value (Figure 2). We have combined viscosity values from two runs performed up to 60 s^{-1} and 100 s^{-1}, which have shown very good agreement. The difference in values between samples with 0.5 wt.%, 1.0 wt.%, and 2.0 wt.% Fe is within the error frame. However, it should be noted that the sample with 2.0 wt.% Fe has shown the highest values. The Fe nanoparticles do not chemically react with flux. It is supposed that the homogeneously distributed Fe nanoparticles in the flux increase the heterogeneity of the size of the particles, which take an active part in internal friction and lead to the viscosity increase. Based on the TEM images and the data sheet of the Fe nanopowder, it is taken that the size of the nanoparticles varies between about 30 nm and 80 nm with the average size of 50 nm.

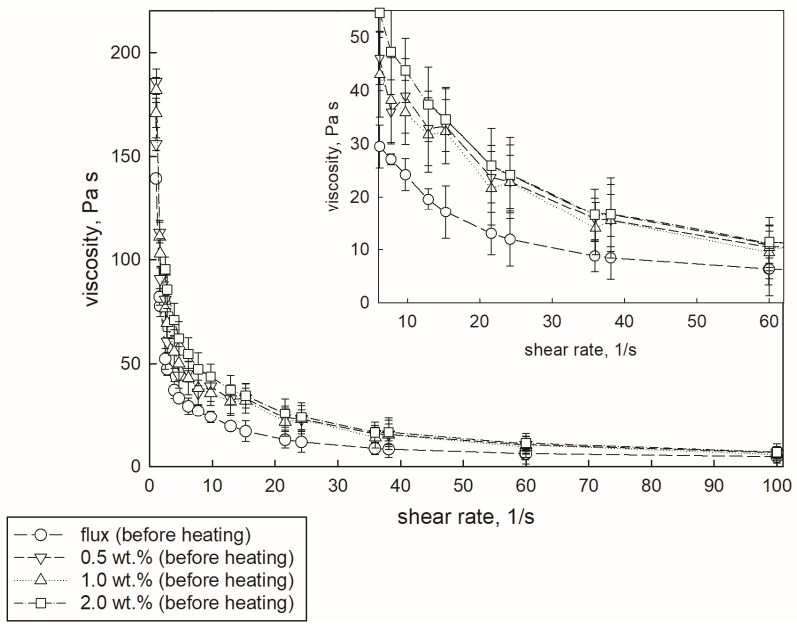


Figure 2. Shear rate dependence of the viscosity for the flux with 0.0 wt.%, 0.5 wt.%, 1.0 wt.%, and 2.0 wt.% of Fe NPs before 1st heating.

The highest values of the viscosity of nanocomposite flux compared to the pure flux remain by heating up to approx. 340 K (Figure 3a–d). We have not seen any difference in values at temperatures higher than 340 K as well as by further cooling and a second run.

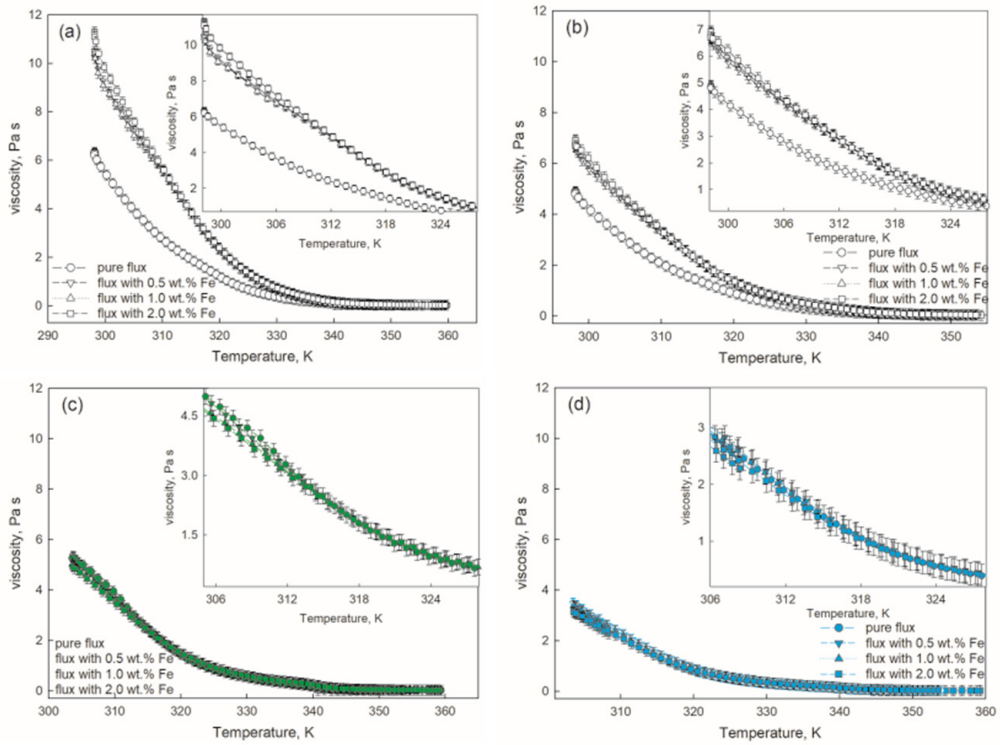


Figure 3. Temperature dependence of the viscosity at 1st heating ((**a**) at shear rate of 60 s^{-1}, and (**b**) at shear rate of 100 s^{-1}), and 2nd heating ((**c**) at shear rate of 60 s^{-1}, and (**d**) at shear rate of 100 s^{-1}) for the flux with 0.0 wt.%, 0.5 wt.%, 1.0 wt.%, and 2.0 wt.% of Fe NPs.

As shown in Figure 4, the highest impact on the viscosity increase was obtained by primary additions of 0.5 wt.% Fe NPs, while we see an insignificant increase in viscosity by further additions of Fe NPs up to 2.0 wt.%. The ratio increases with temperature, while

the absolute value of the viscosity decreases; for instance, it is equal to about 1.3 at room temperature. It can be explained that the structural changes in the flux lead to the viscosity decrease, but the nanoparticle effect remains unchangeable, increasing their impact on the overall internal friction of the samples.

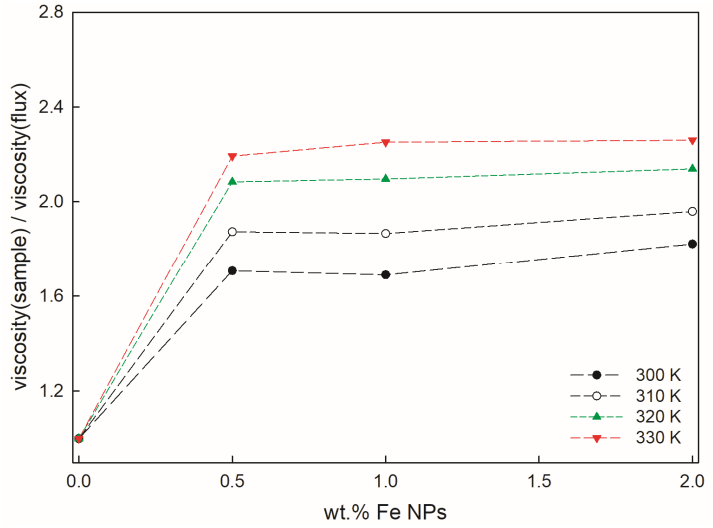


Figure 4. Concentration dependence of the ratio between the viscosity values of the fluxes with Fe NP additions compared to the pure flux.

As shown in Figure 5a–d, the viscosity is practically constant in the range from 360 K to circa 333 K by first cooling and to circa 328 K by second cooling. In general, the viscosity indicates how resistant that fluid is to flow. As the temperature increases, the particles move more quickly in the liquid, having shorter interactions. It leads to the reduction in internal friction, and therefore, the viscosity decreases. It means that within this temperature range, there are no significant changes in the interactions between particles. The viscosity remarkably increases by further cooling up to 323 K, reaching the values obtained by cooling. We can suppose that within the temperature range, there are some structural transformations in the flux leading to an increase in the interaction between particles, making the flux much more viscous; for example, some chemical reactions lead to an increase in the size of the structural units/molecules, which participate in the flux flow. Our experimental results are in good agreement with the technical parameters given by Stannol, who stated that the dropping point of the flux is approx. 323 K [11]. The temperature zone of the significant viscosity increase is between "activation" temperature, at which flux acids as inert compounds break down and form acids, and the dropping temperature of the flux. The viscosity increases continuously by the further cooling starting from about 323 K.

The shear rate dependence of the viscosity from maximum value to minimum at room temperature was investigated at the end of each experiment. The viscosity values from two cooling runs performed starting from 60 s^{-1} and 100 s^{-1} were combined and have shown very good agreement (Figure 6). The absolute viscosity values at higher temperatures after two runs are smaller than at the beginning of the experiments. It could be related to the fact that some part of the sample was flowing out of the disk area, concentrating on the outer zone of the disk bow.

It is well known that abietic acid is widely used to produce flux. There are several studies related to the investigations of the oxidation characteristics of abietic acid. Particularly, it was shown that an oxygen absorption process is relatively low at 333 K, which is a peroxide formation process of abietic acid with oxygen. It was shown that the thermal decomposition of peroxide at the temperature of 353 K would provide lots of free radicals to

accelerate oxidation, leading to the deep radical oxidation of abietic acid with oxygen [12]. It is in agreement with the literature [13], which states that in the first step, peroxide is formed, followed by further oxidation, which forms hydroxyl-containing abietic acid oxide. The differential scanning calorimetry (DSC) test for 7-hydroperoxy-13-abiet-8(14)-enoic acid revealed a major exothermic peak within a temperature range from 313.71 K to 431.10 K and the exothermal onset temperature of 353.94 K [12].

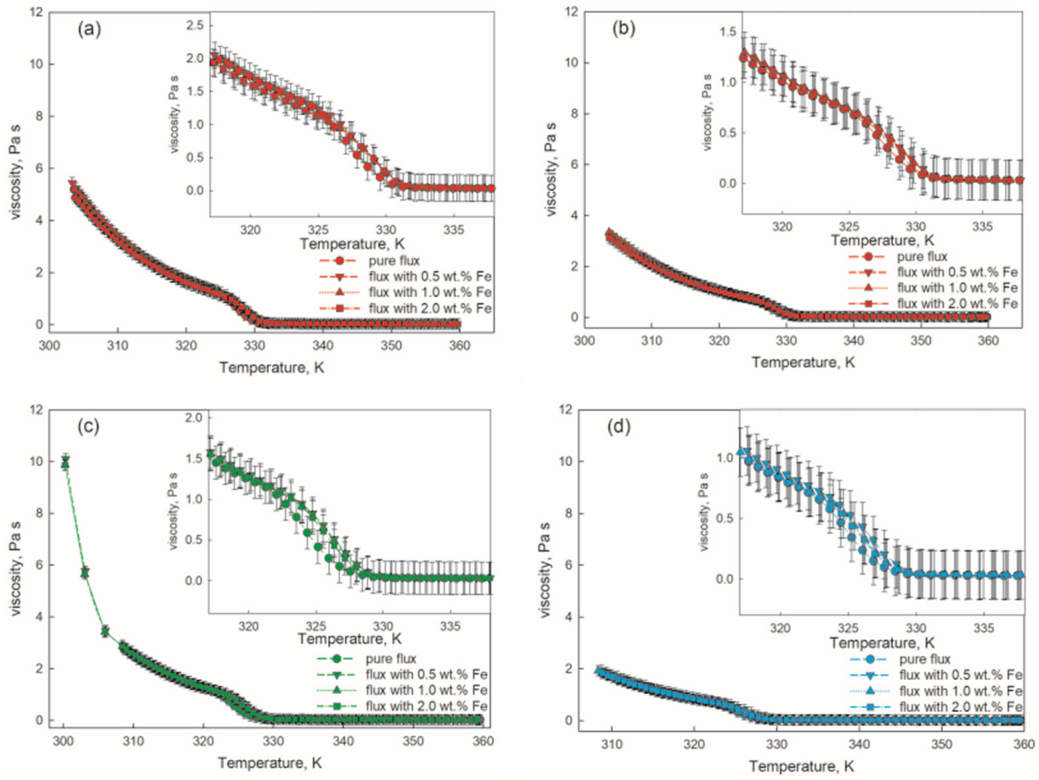


Figure 5. Temperature dependence of the viscosity at 1st cooling ((**a**) at shear rate of 60 s^{-1}, and (**b**) at shear rate of 100 s^{-1}), and 2nd cooling ((**c**) at shear rate of 60 s^{-1}, and (**d**) at shear rate of 100 s^{-1}) for the flux with 0.0 wt.%, 0.5 wt.%, 1.0 wt.%, and 2.0 wt.% of Fe NPs.

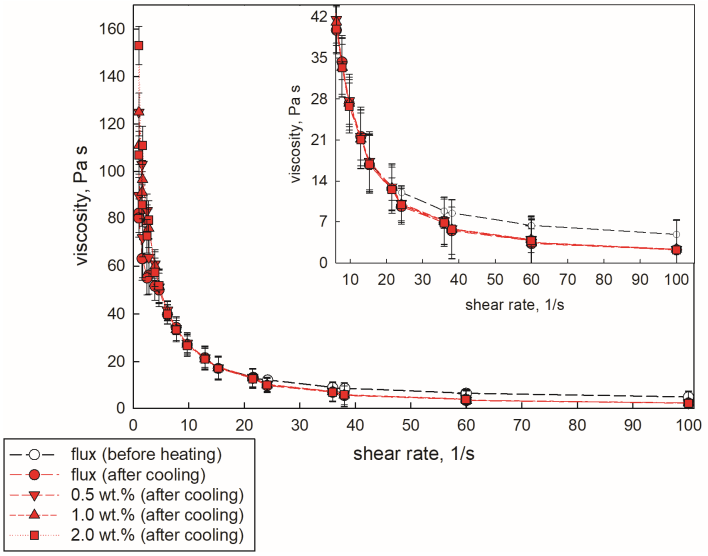


Figure 6. Shear rate dependence of the viscosity for the flux with 0.0 wt.%, 0.5 wt.%, 1.0 wt.%, and 2.0 wt.% of Fe NPs after 2nd cooling.

The performed DTA test of the commercial flux is shown in Figure 7. The exothermic heat effect was obtained during first heating between 314 ± 5 K and 335 ± 5 K. It corresponds to the temperature range with a significant viscosity decrease during the first heating. An exothermic effect by cooling presented in two runs within a temperature range between 330 ± 5 K and 335 ± 5 K is in good agreement with the viscosity results, which have shown a kink in the temperature dependence between approx. 330 K and 335 K. Furthermore, these data match with the literature data of a significant drop in the wetting angle between 318 K and 330 K [10].

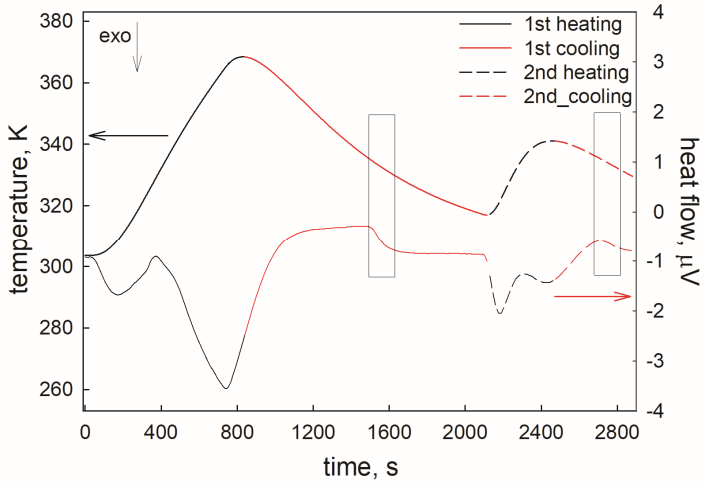


Figure 7. DTA measurements of the commercial flux.

Based on the above presented data, it can be supposed that during a chemical reaction in the flux at about 340 K, the nanosized impurities were precipitated on the bottom disk and did not participate in the internal friction anymore. For this reason, practically no difference in viscosity for the samples with and without minor Fe nanoparticle additions has been observed during both first cooling (Figure 3c,d), second run (Figure 5a–d), and the shear rate decrease in the cooled-down samples (Figure 6). Figure 8 shows the sample on the top plate and the bottom plate.

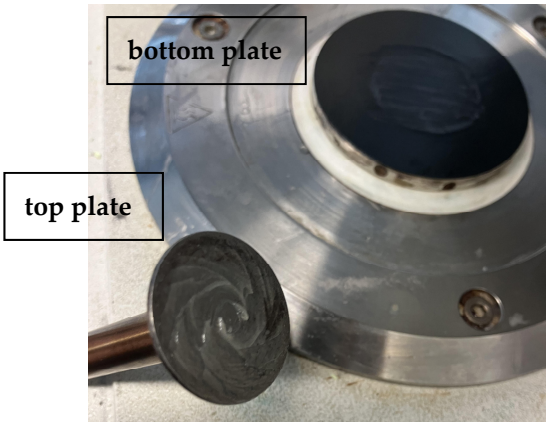


Figure 8. Image of the top and bottom plates with the sample of the viscometer after measurement.

It is shown that the sample part that remained on the top plate is a water-white color, while the sample residues on the bottom plate are black.

4. Conclusions

The minor additions of Fe nanoparticles up to 2.0 wt.% increased the viscosity of the commercial flux Lötfett up to 30% at room temperature. The shear rate dependence has shown a decrease in the viscosity with a rise in the shear rate for all investigated samples, while the relative difference in the absolute values between flux with and without Fe NPs has remained practically the same. The significant viscosity decrease with increased temperature has been shown for all samples in the temperature range between approx. 300 K and 340 K. The viscosity is practically constant by further heating up to 360 K. The drastic viscosity increase during the cooling in the temperature range between circa 330 K and 323 K is in agreement with the DTA results, which have shown an exothermic reaction and could be related with the structural transformation in the investigated flux.

Supplementary Materials: The following supporting information can be downloaded at: https://www.mdpi.com/article/10.3390/met15010093/s1, Figure S1: plate–plate rheometer MCR300; Figure S2: DTA measurement equipment; Table S1: Experimental data of the performed viscosity measurements of the flux during first run at the shear rate of 60 s^{-1}; Table S2: Experimental data of the performed viscosity measurements of the flux during second run at the shear rate of 60 s^{-1}; Table S3: Experimental data of the performed viscosity measurements of the flux during first run at the shear rate of 100 s^{-1}; Table S4: Experimental data of the performed viscosity measurements of the flux during second run at the shear rate of 100 s^{-1}; Table S5: Experimental data of the performed viscosity measurements of the flux with 0.5 wt.% Fe NPs during first run at the shear rate of 60 s^{-1}; Table S6: Experimental data of the performed viscosity measurements of the flux with 0.5 wt.% Fe NPs during second run at the shear rate of 60 s^{-1}; Table S7: Experimental data of the performed viscosity measurements of the flux with 0.5 wt.% Fe NPs during first run at the shear rate of 100 s^{-1}; Table S8: Experimental data of the performed viscosity measurements of the flux with 0.5 wt.% Fe NPs during second run at the shear rate of 100 s^{-1}; Table S9: Experimental data of the performed viscosity measurements of the flux with 1.0 wt.% Fe NPs during first run at the shear rate of 60 s^{-1}; Table S10: Experimental data of the performed viscosity measurements of the flux with 1.0 wt.% Fe NPs during second run at the shear rate of 60 s^{-1}; Table S11: Experimental data of the performed viscosity measurements of the flux with 1.0 wt.% Fe NPs during first run at the shear rate of 100 s^{-1}; Table S12: Experimental data of the performed viscosity measurements of the flux with 1.0 wt.% Fe NPs during second run at the shear rate of 100 s^{-1}; Table S13: Experimental data of the performed viscosity measurements of the flux with 2.0 wt.% Fe NPs during first run at the shear rate of 60 s^{-1}; Table S14: Experimental data of the performed viscosity measurements of the flux with 2.0 wt.% Fe NPs during second run at the shear rate of 60 s^{-1}; Table S15: Experimental data of the performed viscosity measurements of the flux with 2.0 wt.% Fe NPs during first run at the shear rate of 100 s^{-1}; Table S16: Experimental data of the performed viscosity measurements of the flux with 2.0 wt.% Fe NPs during second run at the shear rate of 100 s^{-1}; Table S17: Experimental data of the performed DTA analysis of the commercial flux.

Author Contributions: Conceptualization, A.Y. and G.K.; investigation, A.Y. and I.W.; writing—original draft preparation, A.Y.; writing—review and editing, A.Y., I.W. and G.K.; supervision, G.K.; project administration, G.K.; funding acquisition, G.K. All authors have read and agreed to the published version of the manuscript.

Funding: This research was funded by the Austrian Science Fund (FWF), grant number P 34894. Open Access Funding by TU Wien.

Data Availability Statement: The original contributions presented in this study are included in the article/supplementary material. Further inquiries can be directed to the corresponding author.

Acknowledgments: This research was funded in whole by the Austrian Science Fund (FWF) [10.55776/P34894]. The authors want to thank Peter Svec Sr. from the Department of Physics, Slovak Academy of Sciences for his help with the TEM measurements of the Fe NPs.

Conflicts of Interest: The authors declare no conflicts of interest. The funders had no role in the design of the study; in the collection, analyses, or interpretation of data; in the writing of the manuscript; or in the decision to publish the results.

References

1. Jamshidi, N.; Farhadi, M.; Ganji, D.D.; Sedighi, K. Experimental investigation on the viscosity of nanofluids. *Int. J. Eng.* **2012**, *25*, 201–209. [CrossRef]
2. Saeed, A.; Jawed, M.; Mohsen, S.; Goshtasp, C. The effect of graphene nano-powder on the viscosity of water: An experimental study and artificial neural network modeling. *Nanotechnol. Rev.* **2022**, *11*, 2768–2785. [CrossRef]
3. Yakymovych, A.; Weber, H.; Kaban, I.; Ipser, H. Dynamic viscosity of a liquid Sn-3.0Ag-0.5Cu alloy with Ni nanoparticles. *J. Mol. Liq.* **2018**, *268*, 176–180. [CrossRef]
4. Yalçın, G.; Öztuna, S.; Dalkılıç, A.S.; Wongwises, S. The influence of particle size on the viscosity of water based ZnO nanofluid. *Alex. Eng. J.* **2023**, *68*, 561–576. [CrossRef]
5. Ke, H.; Yuan, M.; Xia, S. A review of nanomaterials as viscosity reducer for heavy oil. *J. Dispers. Sci. Technol.* **2020**, *43*, 1271–1282. [CrossRef]
6. Zhang, L.; Tu, K.N. Structure and properties of lead-free solders bearing micro and nano particles. *Mater. Sci. Eng. R Rep.* **2014**, *82*, 1–32. [CrossRef]
7. Taborda, E.A.; Franco, C.A.; Ruiz, M.A.; Alvarado, V.; Cortés, F.B. Experimental and theoretical study of viscosity reduction in heavy crude oils by addition of nanoparticles. *Energy Fuels* **2017**, *31*, 1329–1338. [CrossRef]
8. Aspalter, A.; Cerny, A.; Göschl, M.; Podsednik, M.; Khatibi, G.; Yakymovych, A.; Plevachuk, Y. Hybrid solder joints: Morphology and shear strength of Sn–3.0Ag–0.5Cu solder joints by adding ceramic nanoparticles through flux doping. *Appl. Nanosci.* **2020**, *10*, 4943–4949. [CrossRef]
9. Wodak, I.; Yakymovych, A.; Khatibi, G. Hybrid solder joints: Morphology and mechanical properties of lead-free Sn-based solders with nano-sized Fe doped flux. In Proceedings of the 2023 46th International Spring Seminar on Electronics Technology (ISSE), Timisoara, Romania, 10–14 May 2023; pp. 1–4. [CrossRef]
10. Wodak, I.; Khatibi, G.; Yakymovych, A.; Krammer, O.; Géczy, A. Iron nanoparticle-doped flux: Wetting characteristics of flux and SAC305 solder and effects on flux viscosity. In Proceedings of the 47th International Spring Seminar on Electronics Technology (ISSE), Prague, Czech Republic, 15–19 May 2024; pp. 1–5. [CrossRef]
11. Available online: https://www.stannol.de/static_data/synology/Datenblaetter____Data%20Sheets/Technical_Data_Sheets____Technische_Datenblaetter/Accessoires____Zubehoer/TDS_Loetfett_DE.pdf (accessed on 22 May 2024).
12. Li, Y.; Xu, X.; Niu, M.; Chen, J.; Wen, J.; Bian, H.; Yu, C.; Liang, M.; Ma, L.; Lai, F.; et al. Thermal stability of abietic acid and its oxidation products. *Energy Fuels* **2019**, *33*, 11200–11209. [CrossRef]
13. Ren, F.; Zheng, Y.-F.; Liu, X.-M.; Yang, Q.-Q.; Zhang, Q.; Shen, F. Thermal oxidation reaction process and oxidation kinetics of abietic acid. *RSC Adv.* **2015**, *5*, 17123–17130. [CrossRef]

Disclaimer/Publisher's Note: The statements, opinions and data contained in all publications are solely those of the individual author(s) and contributor(s) and not of MDPI and/or the editor(s). MDPI and/or the editor(s) disclaim responsibility for any injury to people or property resulting from any ideas, methods, instructions or products referred to in the content.